Astronomical and Astrophysical Transactions (*AApTr*), 2022, Vol. 33, Issue 1, pp. 19–36,
ISSN 1055-6796, Photocopying permitted by license only, ©Cambridge Scientific Publishers

Probable connection between the drag of the International Space Station and various indexes that determine the state of space weather in 23–24 solar activity cycles

V.H. Komendant*

Institute of Radio Astronomy, National Academy of Sciences of Ukraine, 4 Mystetstv Str., Kharkiv, 61002, Ukraine

Received 18 January, 2022

The analysis of the ISS's drag data during the period from 2005 to 2019 was carried out. In the analysis the B-star drag term was applied. This coefficient reflects the influence of changes in the state of the atmosphere on the movement of artificial objects in the Earth's orbit. The time periods of the ISS movement when significant adjustments they were not made to the station's orbit and the reception of planned missions were selected. The analysis of changes in the ISS's drag was carried out. Data of solar and geomagnetic activity, including episodes of strong drag and periods of regular changes were used.

Keywords: ISS, atmosphere, ISS drag, solar activity, geomagnetic activity, space weather

1 Introduction

The International Space Station is an important and unique research facility. Many biological, meteorological, astronomical, physical and cosmological experiments associated with the presence of unique conditions that have no analogues on the Earth's surface are conducted in the station. It is subject to drag due to changes in the density of the atmosphere, like any object launched into low-earth orbit. The position of the station in orbit is constantly monitored and if it is necessary its height is corrected. The change in the ISS altitude occurs as a result of its drag in the Earth's atmosphere, which changes its density under the influence of solar wave and corpuscular activity.

To ensure the safety of the crew and the stability of its orbit the station is continuously monitored. The ISS orbital parameters can be found in the two-line orbital element set (TLE). This format is freely available from NORAD (North American Aerospace Defense Command). These orbital elements are given from three to five times a day (after 5–3 turns of the station around the Earth).

*Email: votan1360@gmail.com

The works about changes in the ISS orbital parameters [1] and episodic changes in the station's orbital period at times of strong solar flare activity (M and X class flares in January 2014) [2] were published in 2014. The first study shows the possible influence of the non-sphericity of the Earth's gravitational field and its compression on some elements of the ISS orbit. In the second, an attempt is made to find out what caused the drag and rise of the station, when the influence of external factors is not obvious. The paper by T. Mendaza et al. – "Influence of interplanetary coronal mass ejection on the density of the thermosphere according to the orbital data of the International Space Station" (2017) [3], provides information about the reaction of the total neutral density of the thermosphere to the impulse effect of solar activity from 2001 to the end of 2006. Their results (obtained by the General Perturbation Method) show that the parameters of the ISS orbit can be used to determine the density of the thermosphere and analyze the solar impact on it.

These three studies reflect the fact that solar and geomagnetic activity significantly affects the state and basic parameters of the Earth's upper atmosphere. In this case, the influence of solar activity is manifested in two main factors: wave radiation and corpuscular flows. However, a complete analysis of the periodic and anomalous decelerations of the ISS has not yet been carried out.

In this paper, the International Space Station (ISS) is used as an indicator of the impact of space weather on the Earth's upper atmosphere [4, 5].

2 Data used

The ISS is a manned station with a mass of 418 tons and a length of 109 meters, located at an altitude of about 400 km. Its orbital inclination $i = 51.6°$; the value of the eccentricity of the orbit $e = 0.00037$; the average values of the minimum and maximum distances from the Earth's surface $r_{min} = 372$ km and $r_{max} = 382$ km.

These observations cover the period of a prolonged minimum at the end of the 23rd solar cycle, the growth, maximum and decline phases of cycle 24 (04.03.2005–31.12.2019). The B-star drag coefficient (drag term) is used in this work. This coefficient is used in the SGP and SDP models to take into account the atmospheric drag on the satellite motion and illustrates the satellite's susceptibility to atmospheric drag in orbit [6].

SGP models are applied to objects near the Earth with orbital periods of less than 225 min. These models take into account the influence of perturbations caused by the shape of the Earth, the resistance of the atmosphere and radiation from the Sun [7, 8]. The SDP models are applied to objects with orbital periods greater than 225 min that correspond to the altitude of 5877.5 km, assuming a circular orbit. These models take into account the gravitational perturbations caused by some other objects such as the Sun and the Moon [7, 8].

Since the solar wave and corpuscular radiation increase the temperature of the atmosphere, the density increases in its higher layers, therefore, the drag force affecting the satellite increases.

In these models the ballistic coefficient B is calculated by the formula:

$$B = \frac{C_D \cdot A}{m},$$

where B – the ballistic coefficient, C_D – the aerodynamic drag coefficient. If the mean free path of air molecules is much larger than the geometric size of the satellite, then C_D is close to 2, A – the midsection area (cross-sectional area of the satellite), m – the satellite mass.

The B-star drag term coefficient is related to the ballistic coefficient by the formula:

$$B^* = B \cdot \frac{\rho_0}{2},$$

where B^* – the modified ballistic coefficient or B-star drag term, B – the ballistic coefficient, ρ_0 – some standard density value for a given altitude. The B-star drag term coefficient has the dimension of $1/R_E$, where $R_E = 6\ 371$ km is the radius of the Earth.

A number of difficulties arise, some of which are associated with the calculation of the atmospheric wind speed perpendicular to the cross-sectional area of the satellite, and the impossibility of accurately taking into account the C_D parameter. Thus, all models, when estimating the B parameter, correct it so that the calculated parameters correspond to the observed positions of the object in the best way. For this reason, this work uses just this coefficient. The coefficient reflects only the atmospheric effect on the object under study [9].

In [10–13], this coefficient is used to analyze the drag of artificial objects under various states of solar and geomagnetic activity.

Many factors of gravitational and non-gravitational nature affect the flight of artificial objects in near-Earth orbit. In this work, the factors associated with the gravitational nature are excluded by choosing the B-star coefficient as the analyzed parameter. Solar and geomagnetic activity have a significant impact on the change in the satellites orbit among the disturbing factors of a non-gravitational nature.

The wide range of indices reflecting the state of space weather are used in this work: W – Wolf numbers; S_p – the total area of the sunspots, $F_{10.7}$ – the radio emission from the Sun at a wavelength of 10.7 cm, TSI (total solar irradiance) – the solar constant, L_α – the Lyman alpha radiation, E – the fluxes of electrons with energies greater than 0.6 MeV and 2 MeV, the solar wind parameters, IMF – the interplanetary magnetic field, A_p – the planetary geomagnetic index, D_{st} (Disturbance Storm Time Index) – the index of the intensity of geomagnetic storms.

The Wolf number and the total area of the sunspots characterize the 11-year cycle of solar activity.

The $F_{10.7}$, TSI and L_α indexes characterize the wave component of the solar ionization radiation.

The radio emission from the Sun at a wavelength of 10.7 cm, $F_{10.7}$, characterizes the wave flux, which correlates with the ultraviolet and the X-ray fluxes of the Sun.

The TSI is a measure of the amount of solar energy received by a body located at a certain distance from the Sun. For the Earth, TSI is defined as the solar energy received per unit area in the upper atmosphere with an average distance from the Earth to the Sun equal to 1 AU. The TSI is approximately 1.35 kW/m^2. This "constant" changes every day, as does the sunspot activity, and over longer periods of time depending on the solar cycle. This constant reflects the change in the total energy flux of solar radiation.

The Lyman alpha radiation, L_α, is a spectral series in the spectrum of the hydrogen atom, was named after the physicist Theodore Lyman, who discovered this series

in 1906. The series is formed during transitions of electrons from the high energy levels to the first one in the emission spectrum and from the first level to all others during absorption. At normal conditions, L_α is located in the ultraviolet region of the spectrum.

The electron fluxes with energies greater than 0.6 MeV and 2 MeV, E, and the solar wind parameters reflect the corpuscular component of the Sun's activity. They reflect the effect on ionospheric currents, which forms the magnetosphere.

The indexes IMF, A_p, and D_{st} show the disturbance of the interplanetary environment, the magnetosphere reaction to changes in the conditions in the interplanetary environment, and the intensity of disturbances in the magnetosphere, respectively.

The interplanetary magnetic field, IMF, is a component of the solar magnetic field, which is pulled from the solar corona by the flow of the solar wind and fills the solar system.

The planetary geomagnetic index, A_p, characterizes the degree of the solar activity effect on the magnetosphere.

To analyze the magnetic storms, the D_{st} index is used. It is an axisymmetric component of the perturbed magnetic field with respect to the geomagnetic dipole and is determined on the basis of magnetic field measurements at four near-equatorial stations: San Juan, Hermanus, Kakioka, Honolulu.

A detailed graph of the change in the drag coefficient for the period 2005 is shown in Fig. 1. It shows a character of the change in the value of the B-star coefficient.

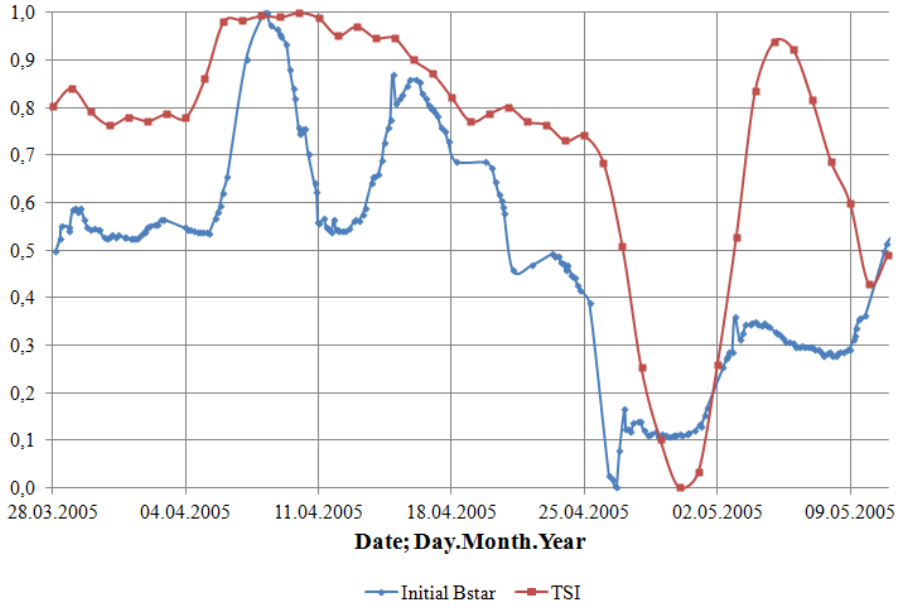


Figure 1 Changes in the initial values of the ISS's drag coefficient (B-star) and the solar constant for the period 28.03.2005–11.05.2005 (the trend has not been subtracted, the values are normalized on maximum value in this period at axis Y). The B-star coefficient data was taken from the archive (https://celestrak.com/NORAD/archives/).

The drag of the ISS as an object for analysis is very specific. It can be seen from these data. Its height is regularly corrected in addition to evasive maneuvers of the station and docking with it of planned missions.

The time periods between two successive corrections of the altitude of the international station were selected for the analysis. These periods have as few maneuvers as possible. The longest periods between the ISS orbit adjustments were selected. As a result, five periods were obtained for analysis: 1) 28.03.2005–11.05.2005; 2) 16.01.2009–17.03.2009; 3) 31.03.2009–28.06.2009; 4) 15.09.2012–04.10.2012; and 5) 03.11.2012–16.12.2012.

3 The anomalous drag periods of the ISS and the state of space weather

3.1 28.03.2005–11.05.2005

This period is characterized by three significant events of increased drag: April 4–8; April 11–15 and April 29 – May 3. These events are shown in Fig. 1. It shows the initial values of the ISS's drag coefficient.

Three C class flares were observed from 4 to 8 April. This maximum can be associated with the combined effect of the co-rotating interaction region (CIR) and the high-speed flow from a coronal hole in the geoeffective position. These events led to an increase in the parameters of the solar wind and geomagnetic activity (A_p = 48, K_p = 5–7). The high-speed flow of the coronal hole was no longer geoeffective by April 7.

The C class flares and the geoeffective flow from the coronal hole were recorded on April 11–15. The high-speed flow from the coronal hole caused geomagnetic disturbances at mid-latitudes on April 11–13 (A_p = 30–26, K_p = 4–6). The crossing of the border of the solar sector was also recorded on this day. This event was accompanied by an increase in the parameters of the solar wind and interplanetary magnetic field.

The solar activity was at a low level during the period from April 29 to May 3. Up to 17 class C flares were observed. This period is caused by a high-speed flow from the geoeffective coronal hole. This flow also caused an increase in geomagnetic activity from April 29 to May 1 (A_p = 21–36, K_p = 4–6).

To calculate the correlation coefficients between the drag coefficient of the International Space Station and the indexes of solar and geomagnetic activity the interpolated data were used. The cubic B-spline method was applied with a step of one day. During this observation period, the highest correlation coefficient (0.69) of the B-star with the TSI index, when the trend has not been subtracted from the data (Fig. 1).

The correlation coefficient of the solar constant with the B-star becomes insignificant (0.16) after subtracting the trend component from the data. The correlation of the drag coefficient with the Lyman alpha index (0.31) and electron fluxes with energies greater than 0.6 MeV (0.52) increases (Fig. 2). Based on the correlation coefficients and the plotted graphs, the long-period component of the change in the ISS's drag coefficient reflects the change in the TSI index, and the short-period component reflects the change in the high-energy electrons fluxes.

The B-star correlation coefficients with the indices of solar and geomagnetic activity for the periods of increased drag of the ISS were also calculated. The trend was

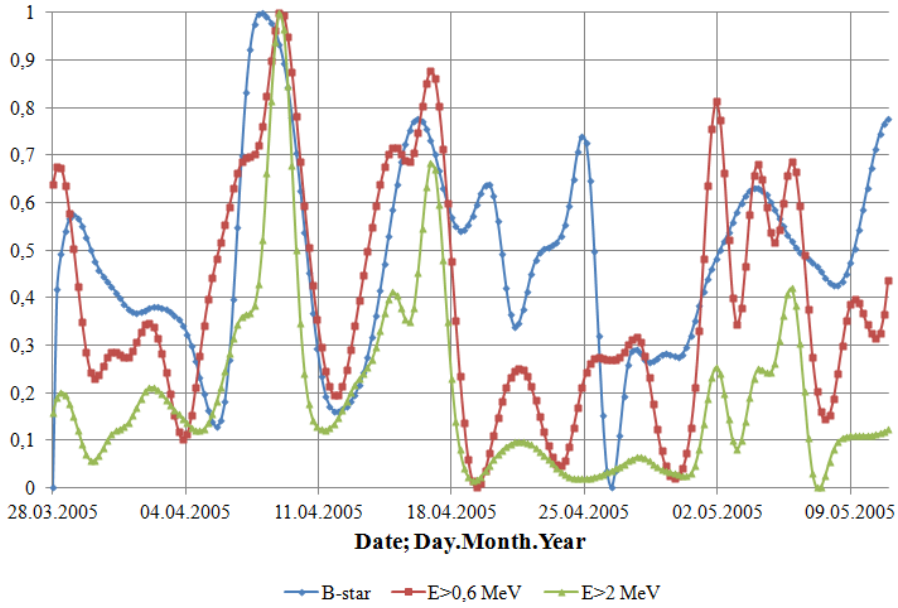


Figure 2 Changes in the values of the ISS's drag coefficient (B-star) and the electron fluxes with the energies greater than 0.6 and 2 MeV for the period 28.03.2005–11.05.2005 (the trend is subtracted, the values are normalized on maximum value in this period at axis Y).

Date			Ap	E>0,6 MeV	E>2 MeV	RadioFlux10.7cm	Sp Total	W	Proton density	Flow speed	Flow pressure	IMF	Dst	Lα	TSI
04.04.2005	11.04.2005	B-star	-0,52	0,84	0,78	-0,23	0,19	0,04	-0,19	-0,62	-0,75	-0,55	0,37	0,59	0,46
11.04.2005	18.04.2005	B-star	-0,76	0,75	0,66	0,38	0,24	0,53	-0,44	-0,31	-0,89	-0,69	0,41	0,09	-0,14
29.04.2005	08.05.2005	B-star	-0,28	0,77	0,59	-0,06	-0,03	-0,09	-0,38	-0,34	-0,56	-0,61	0,10	0,77	0,76

Figure 3 The table of the correlation coefficient values for the periods of increased drag of the ISS (the trend is subtracted).

subtracted from the data before that. These coefficients are presented in the table in Fig. 3. The highest correlation coefficients between B-star and electron fluxes with energies greater than 0.6 and 2 MeV (0.66–0.84) were for two events of increased drag of the ISS (April 4–8 and April 11–15). For the April 29 – May 3 event, the highest correlation coefficients are between B-star, L_α (0.77) and TSI (0.76).

Analysis of the initial data and data with the subtracted trend makes it possible to estimate the duration of the perturbations in the movement of the ISS caused by the selected indexes. It allows us to make the conclusion about which of the indexes of solar or geomagnetic activity determine the main tendency of changes in the ISS's orbital motion at the selected study interval, and which ones supplement their influence.

3.2 16.01.2009–17.03.2009

This period, shown in Fig. 4, contains 5 events of increasing drag: January 20–21; January 26–29; February 13–18; February 21 – March 3; March 5–7.

Solar activity was at low level on January 20–21. The geoeffective high-velocity flow from the coronal hole was recorded during this time period. The same flow caused a geomagnetic disturbance at all latitudes on January 19 ($A_p = 9$, $K_p = 4$).

No strong solar activity was recorded in the period from January 26 to January 29. Geomagnetic disturbances at high latitudes ($A = 22$, $K = 6$) were recorded on January 26. The reason for this was the south-oriented Bz component of the interplanetary magnetic field (IMF) in combination with the high-speed flow of the coronal hole.

The period of February 13–18 is associated with low flare activity on February 10–13 (B class flares), the joint influence of the high-speed flow from the coronal hole and the co-rotating interaction region (February 14). These events resulted in an increase in the parameters of the solar wind, IMF, and an increase in geomagnetic activity at high latitudes on February 14–15 ($A = 25$, $K = 6$).

No flare activity was observed on February 21 – March 3. This event could have been caused by a high-speed coronal hole flow, which caused geomagnetic disturbances at high latitudes on February 27–28 ($A = 20$, $K = 6$).

The event of March 5–7 cannot be connected with the phenomena of solar activity. Solar activity was low (no flares were recorded). Perhaps this event was the reaction

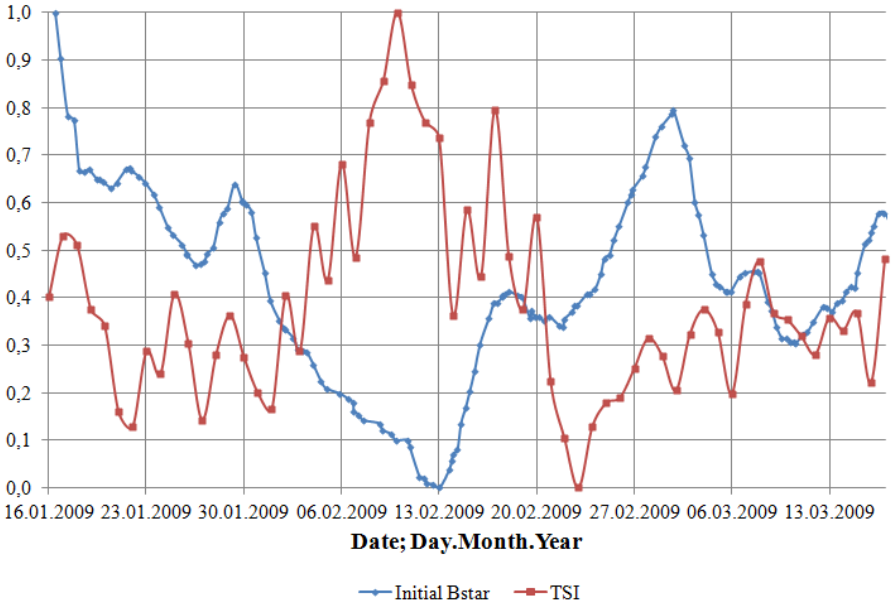


Figure 4 Changes in the initial values of the ISS's drag coefficient (B-star) and the solar constant for the period 16.01.2009–17.03.2009 (the trend has not been subtracted, the values are normalized on maximum value in this period at axis Y). The B-star coefficient data was taken from the archive (https://celestrak.com/NORAD/archives/).

to the change in the solar wind speed, which caused a weak geomagnetic disturbance on March 3 ($A_p = 5$, $K_p = 3$).

The correlation coefficients between B-star and the indexes of solar and geomagnetic activity are insignificant for data that did not take into account the trend. The TSI index with the ISS's drag coefficient has the correlation coefficient of –0.59 (Fig. 4). The highest correlation coefficient B-star shows with the indexes of electron fluxes with energies greater than 0.6 MeV (0.41) and 2 MeV (0.40) for the data with subtracting the trend component (Fig. 5).

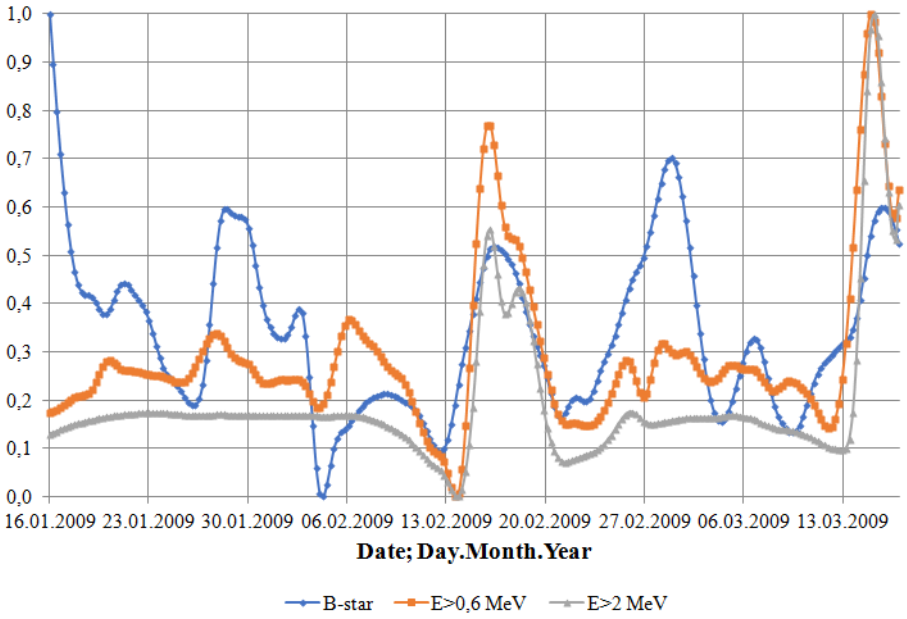


Figure 5 Changes in the values of the ISS's drag coefficient (B-star) and the electron fluxes with the energies greater than 0.6 and 2 MeV for the period 16.01.2009–17.03.2009 (the trend is subtracted, the values are normalized on maximum value in this period at axis Y).

We can conclude that the short-period changes in the ISS's drag were caused by changes in the electron flux indices (>0.6 MeV and >2 MeV) based on the correlation coefficients and the plotted graphs. We did not find the indexes that could cause the long-period components of the drag in the given observation interval.

The B-star correlation coefficients with the indexes of solar and geomagnetic activity calculated for the periods of intensified drag of the ISS (before that the trend was subtracted from the data) are shown in the table in Fig. 6. The highest correlation coefficients between B-star and electron fluxes with energies above 0.6 and 2 MeV (0.38–0.93) are for three events of enhanced drag of the ISS (January 26–29; February 13–18; February 21 – March 3). For the March 5–7 event, the highest correlation coefficients are between B-star and W (0.81), S_p (0.81), D_{st} (0.74) indexes. The correlation coefficients of the B-star with electron fluxes with energies greater than 0.6 and 2 MeV were 0.93 and 0.90, respectively, during the period of increasing drag of the ISS on February 13–18.

Date			Ap	E>0,6 MeV	E>2 MeV	RadioFlux10.7cm	Sp Total	W	Proton density	Flow speed	Flow pressure	IMF	Dst	Lα	TSI
20.01.2009	26.01.2009	B-star	-0,65	0,29	0,09	-0,69	-0,53	-0,55	-0,69	0,34	-0,59	-0,65	-0,22	-0,19	-0,62
27.01.2009	13.02.2009	B-star	-0,38	0,38	0,40	-0,25	-0,44	-0,44	-0,43	0,38	-0,28	0,04	0,36	-0,42	-0,29
13.02.2009	20.02.2009	B-star	-0,32	0,93	0,90	0,29	-0,17	-0,13	-0,79	0,32	-0,73	-0,61	-0,51	0,83	0,29
20.02.2009	06.03.2009	B-star	0,01	0,66	0,47	-0,32	0,03	0,00	-0,55	0,28	-0,44	-0,49	-0,06	0,16	0,33
05.03.2009	11.03.2009	B-star	0,03	0,02	0,23	0,55	0,81	0,81	0,58	-0,11	0,35	0,33	0,74	-0,16	-0,28

Figure 6 The table of the correlation coefficient values for the periods of increased drag of the ISS (the trend is subtracted).

3.3 31.03.2009–28.06.2009

This time interval (Fig. 7) includes three events which caused an increase in ISS's drag: April 7–10, April 16–22, May 13–18.

No sunspots and flare activity were observed on April 7–10. This period is caused by the high-speed flow from the coronal hole. It caused the increase in solar wind parameters by the end of April 8 and the increase in geomagnetic activity at high latitudes on April 11 ($A = 16$, $K = 5$).

The increase of the drag on April 16–22 was caused by the high-speed flow from the coronal hole, which was recorded on April 16. There was no flare activity, and the visible solar disk was spotless. The high-speed flow caused an increase in geomagnetic activity at high latitudes ($A = 13$, $K = 4$) and the increase in the solar wind parameters on April 16. The perturbations caused by the flow of the coronal hole subsided by April 18–19, but the period of enhanced drag lasted until April 22.

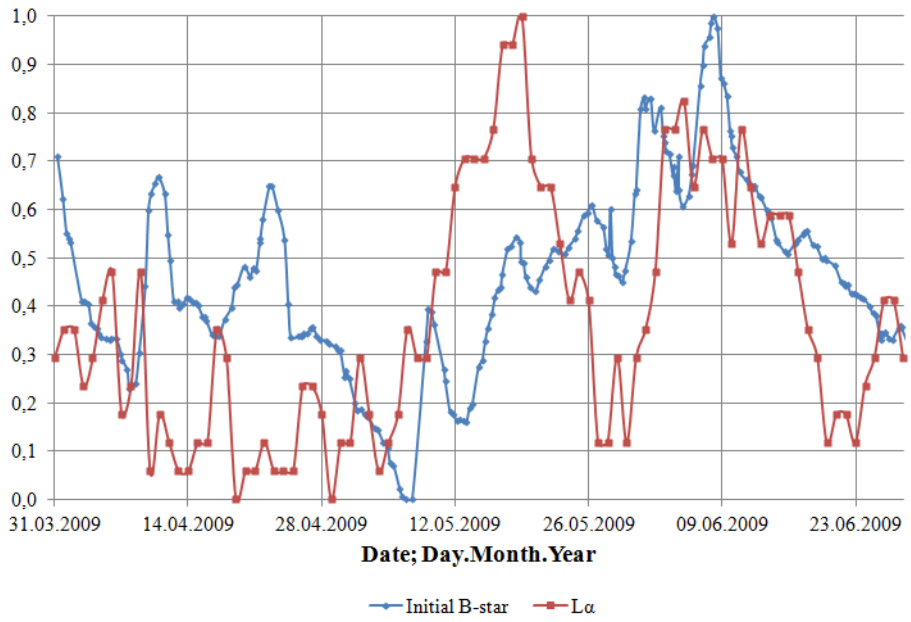


Figure 7 Changes in the initial values of the ISS's drag coefficient (B-star) and the L_α index for the period 31.03.2009–28.06.2009 (the trend has not been subtracted, the values are normalized on maximum value in this period at axis Y). The B-star coefficient data was taken from the archive (https://celestrak.com/NORAD/archives/).

The period May 13–18 was the result of changes in solar wind parameters caused by crossing the solar sector boundary on May 14. These events caused an increase in geomagnetic activity on May 14 ($A_p = 8$, $K_p = 4$).

The shock wave is recorded on May 28. It is accompanied by an increase in solar wind parameters and, as a result, an increase in geomagnetic activity at high latitudes at the same day ($A = 9$, $K = 4$). Perhaps the period May 28–31 was caused by an interplanetary shock wave.

The periods of drag after May 31 could not be associated with the phenomena of solar and geomagnetic activity.

Correlation coefficients for a given observation interval are insignificant. The highest correlation coefficients of the ISS's drag with indices L_α (0.32) (Fig. 7) and S_p (0.31) at the minimum of solar activity at the end of March – June 2009 for data with an unaccounted trend.

The values of the correlation coefficients for the L_α (–0.11) and S_p (0.21) indexes with B-star fall after taking into account the trend component in the data (Fig. 8). The rest of the indexes, as well as for the data with the subtracted trend, do not show significant correlation coefficients.

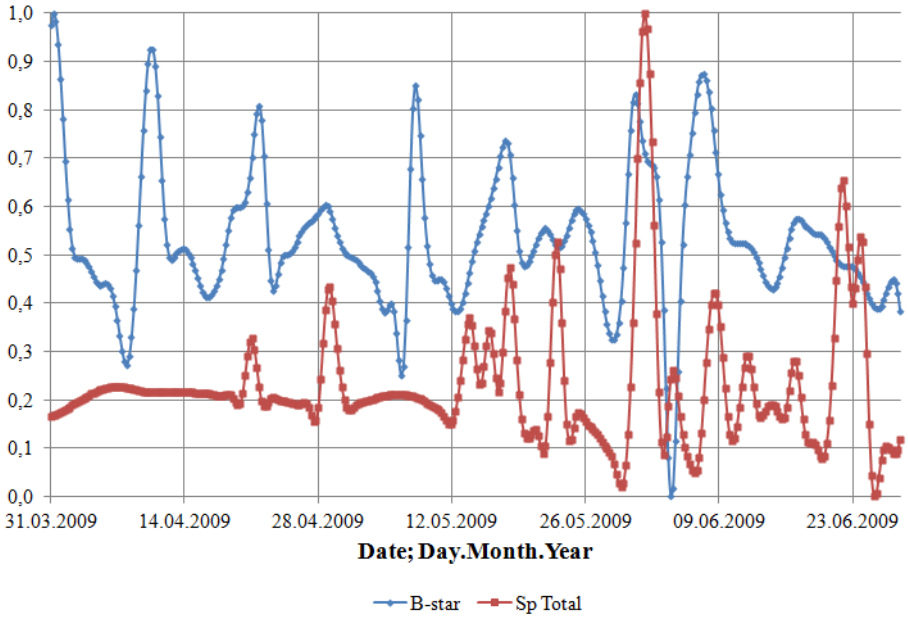


Figure 8 Changes in the values of the ISS's drag coefficient (B-star) and the S_p index for the period 31.03.2009–28.06.2009 (the trend is subtracted, the values are normalized on maximum value in this period at axis Y).

The B-star correlation coefficients with the solar and geomagnetic activity indexes calculated for the periods of intensified drag of the ISS (before that the trend was subtracted from the data) are shown in the table in Fig. 9. For three events of enhanced drag of the ISS (April 16–22; May 30 – June 5; June 5–17) the highest correlation coefficients between B-star and electron fluxes with energies above 0.6

Date			Ap	E>0,6 MeV	E>2 MeV	RadioFlux10.7cm	Sp Total	W	Proton density	Flow speed	Flow pressure	IMF	Dst	Lα	TSI
07.04.2009	12.04.2009	B-star	0,41	0,32	0,00	-0,54	-0,79	-0,78	-0,74	0,91	-0,19	0,17	-0,64	-0,33	-0,76
16.04.2009	25.04.2009	B-star	-0,32	0,49	0,44	0,42	0,47	0,47	-0,63	0,17	-0,47	-0,39	-0,32	-0,40	-0,15
13.05.2009	21.05.2009	B-star	-0,50	-0,55	-0,58	0,15	0,41	0,23	-0,60	0,33	-0,45	-0,67	-0,25	0,51	0,22
21.05.2009	29.05.2009	B-star	-0,54	0,53	0,44	0,33	0,35	0,36	-0,31	-0,59	-0,46	-0,47	0,39	0,58	0,57
30.05.2009	05.06.2009	B-star	-0,82	0,85	-0,07	0,00	0,46	0,06	-0,30	0,00	-0,15	-0,84	0,34	-0,73	-0,55
05.06.2009	17.06.2009	B-star	0,06	0,81	-0,50	-0,36	0,08	-0,42	-0,43	0,43	-0,17	0,06	-0,26	0,10	0,52

Figure 9 The table of the correlation coefficient values for the periods of increased drag of the ISS (the trend is subtracted).

MeV (0.49–0.85). For the April 7–10 event, the highest correlation coefficients are between B-star and solar wind speed (0.91). During the period of increasing drag of the ISS on May 13–21 and May 21–27, the B-star correlation coefficients have the highest values with L_α (0.51–0.58) and TSI (0.57).

3.4 15.09.2012–04.10.2012

A lot of maneuvers and undocking of planned missions were carried out during this period, so it was possible to single out only one event of enhanced drag on September 19–26 (Fig. 10).

20 C class flares have been reported during this period. This event was caused by the arrival in the near-Earth space of the geoeffective co-rotating interaction region.

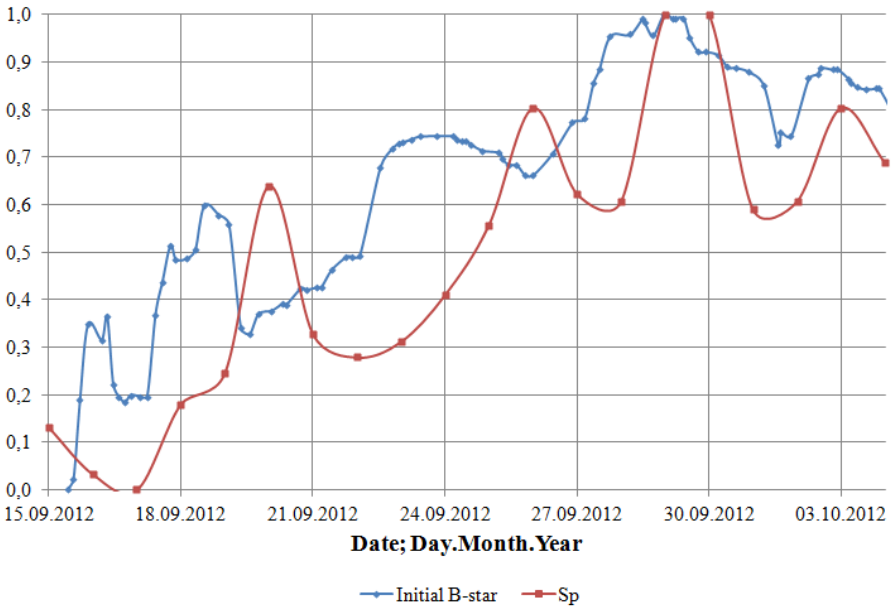


Figure 10 Changes in the initial values of the ISS's drag coefficient (B-star) and the S_p index for the period 15.09.2012–04.10.2012 (the trend has not been subtracted, the values are normalized on maximum value in this period at axis Y). The B-star coefficient data was taken from the archive (https://celestrak.com/NORAD/archives/).

It caused the increase in geomagnetic activity on September 19 ($A_p = 14$, $K_p = 4$), which continued at high latitudes from September 18 to 22 ($A = 15$–20, $K = 3$–5). The border of the solar sector containing the geoeffective coronal hole is crossed on September 20.

Two shock waves were recorded on September 30. They are associated with the arrival of a coronal mass ejection (CME). The space station did not respond to these phenomena. This may be due to the undocking of the planned mission on September 28 and subsequent maneuvers of the station.

The main indexes influencing the ISS's drag with the highest correlation coefficients, for the initial data, at the phase of the first maximum of the 24 solar cycle activity 15.09.2012–04.10.2012 were: S_p (0.79) (Fig. 10); L_α (0.76); $F_{10.7}$ (0.75).

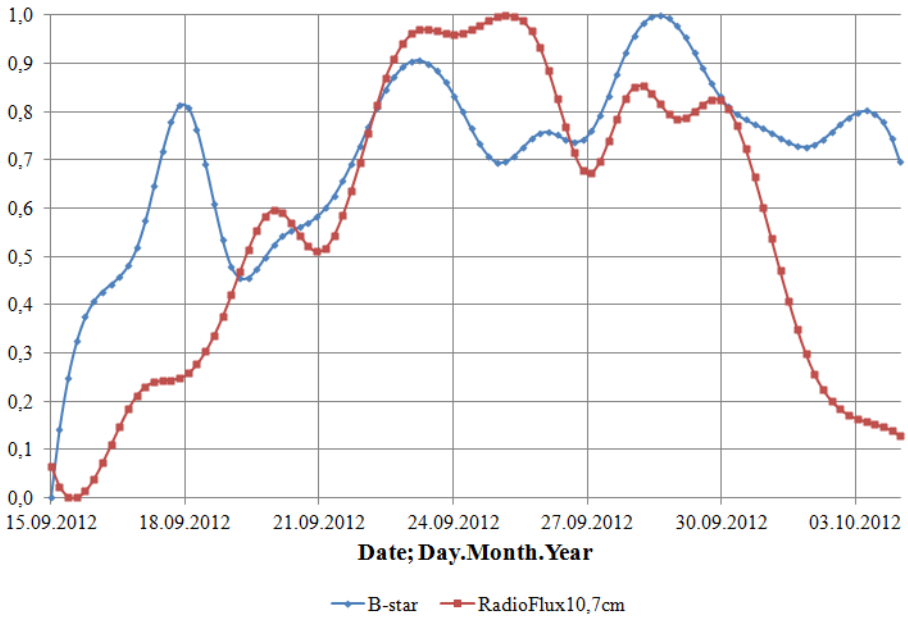


Figure 11 Changes in the values of the ISS's drag coefficient (B-star) and the $F_{10.7}$ index for the period 15.09.2012–04.10.2012 (the trend is subtracted, the values are normalized on maximum value in this period at axis Y).

Due to the exclusion of the trend component it was revealed that the $F_{10.7}$ and L_α indexes also affect the appearance of short-period variations in the ISS's drag for the period 15.09.2012–04.10.2012 (Fig. 11).

Date			Ap	E>0,6 MeV	E>2 MeV	RadioFlux10.7cm	Sp Total	W	Proton density	Flow speed	Flow pressure	IMF	Dst	Lα	TSI
19.09.2012	26.09.2012	B-star	-0,65	0,61	0,68	0,82	-0,55	-0,11	-0,21	-0,53	-0,71	-0,49	0,72	0,62	-0,39

Figure 12 The table of the correlation coefficient values for the periods of increased drag of the ISS (the trend is subtracted).

The correlation coefficients of B-star with the indexes of solar and geomagnetic activity calculated for the period of intensification of the ISS's drag (before that the trend was subtracted from the data) are shown in the table in Fig. 12. The highest correlation coefficients between B-star with indices $F_{10.7}$ (0.82) and D_{st} (0.72). Correlation coefficients of B-star with electron fluxes with energies higher than 0.6 MeV – 0.68; 2 MeV – 0.61 and L_{α} – 0.62.

3.5 03.11.2012–16.12.2012

This period is shown in Fig. 13. It contains three events of increased drag: November 8–17, November 29 – December 1, December 3–5.

The November 8–17 event was caused by the combined influence of: crossing the solar sector boundary on November 6 with the corresponding increase in solar wind parameters; geoeffective CIR (November 6); high-speed coronal hole flow (November 6); long flares of M1 (November 8 and 11) and C2 (November 10) class; geoeffective CME associated with the C class flare on November 10; M2 (this flare was associated with an increase in the $F_{10.7}$ index) and M6 class flares on November 13; crossing the border of the solar sector on November 14 with the geoeffective coronal hole.

The November 29 – December 1 event was most likely caused by M1 and M2 class flares. As a result of the CME arrival (which occurred on November 9 and 10), the

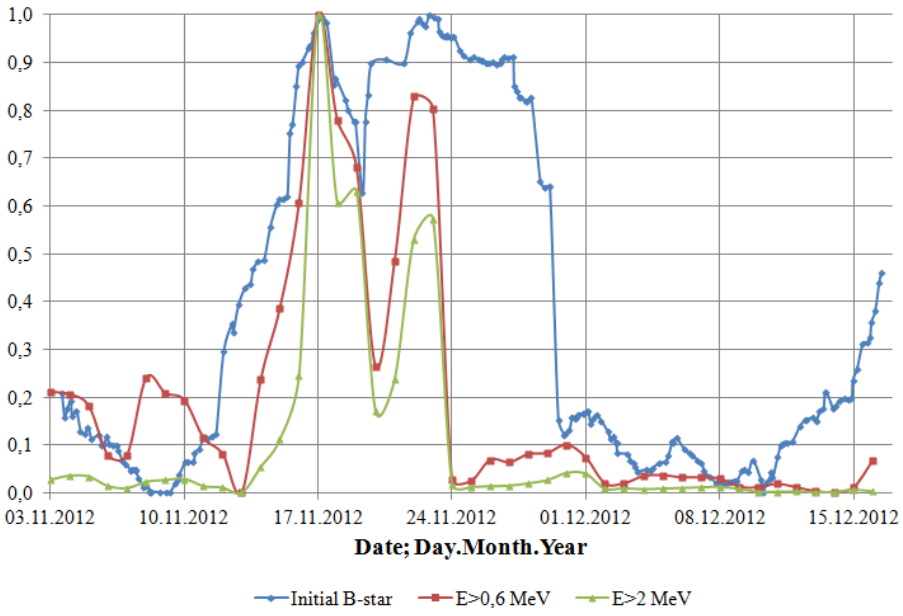


Figure 13 Changes in the initial values of the ISS's drag coefficient (B-star) and the electron fluxes with energies greater than 0.6 and 2 MeV for the period 03.11.2012–16.12.2012 (the trend has not been subtracted, the values are normalized on maximum value in this period at axis Y). The B-star coefficient data was taken from the archive (https://celestrak.com/NORAD/archives/).

geomagnetic storm was recorded on November 13 ($A_p = 15$, $K_p = 4$) and November 14 ($A_p = 44$, $K_p = 7$).

The increase in the drag coefficient on December 3–5 could be caused by a high-speed flow of the coronal hole (December 4), due to solar activity which was at a low level (in total, three C class flares; the most powerful of which is the C3 flare).

The period from November 19 to November 28 is not considered. The planned mission and possibly the station maneuvers associated with this event were held on November 18 (this means that the station height was changed artificially).

In the period 03.11.2012–16.12.2012, for the initial data, the highest correlation coefficients with the B-star were for the electron flux indexes >0.6 MeV and >2 MeV (0.66) (Fig. 13), as well as the Lyman alpha index (0.62). The high correlation coefficients also had indexes: $F_{10.7}$ (0.58); W (0.56); Flow speed (0.54).

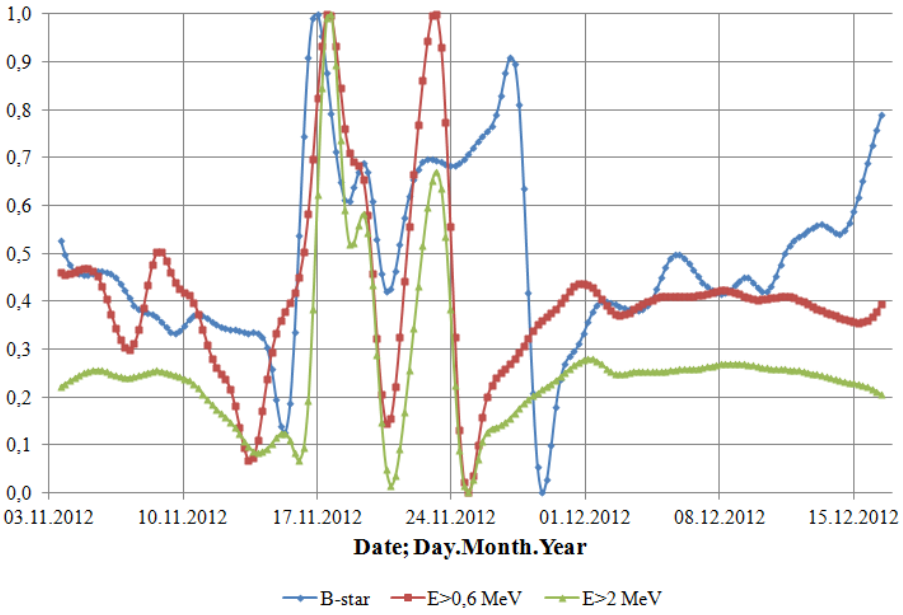


Figure 14 Changes in the values of the ISS's drag coefficient (B-star) and the electron fluxes with energies greater than 0.6 and 2 MeV for the period 03.11.2012–16.12.2012 (the trend is subtracted, the values are normalized on maximum value in this period at axis Y).

The exclusion of the trend component from the initial data (Fig. 14) (for the period 03.11.2012–16.12.2012) showed that the correlation coefficients of the B-star with the indexes of solar and geomagnetic activity became insignificant. The highest values of the correlation coefficients were for the electron flux indexes >2 MeV (0.37) and >0.6 MeV (0.34). In the same range were the values of the correlation coefficients for the indexes: TSI (0.31); solar wind flow velocity (0.24) and Lyman alpha (0.22).

The B-star correlation coefficients with the solar and geomagnetic activity indexes calculated for the periods of intensified drag of the ISS (before that the trend was subtracted from the data) are shown in the table in Fig. 15. The highest correlation coefficients between B-star and electron fluxes with energies greater than 0.6 MeV (0.54–0.78) and 2 MeV (0.51–0.75) for two events of enhanced drag of the ISS

Date			Ap	E>0,6 MeV	E>2 MeV	RadioFlux10.7cm	Sp Total	W	Proton density	Flow speed	Flow pressure	IMF	Dst	Lα	TSI
08.11.2012	19.11.2012	B-star	-0,23	0,78	0,75	-0,11	-0,13	0,34	-0,45	0,13	-0,26	-0,20	0,26	0,38	0,51
19.11.2012	29.11.2012	B-star	0,13	0,07	0,11	-0,23	-0,68	-0,56	0,12	0,28	0,28	0,05	0,10	-0,18	-0,18
29.11.2012	03.12.2012	B-star	0,62	-0,03	0,51	-0,80	-0,95	-0,88	0,81	-0,04	0,76	0,38	-0,05	-0,72	-0,68
03.12.2012	08.12.2012	B-star	-0,48	0,54	0,13	0,07	0,10	0,08	-0,53	0,15	-0,77	-0,68	-0,38	0,17	0,50

Figure 15 The table of the correlation coefficient values for the periods of increased drag of the ISS (the trend is subtracted).

(November 8–17, December 3–5). For the November 29 – December 1 event, the B-star has the highest correlation coefficients with the proton density (0.81), solar wind pressure (0.76) and A_p (0.62). The B-star has also high correlation coefficients with TSI in the period of intensification of ISS's drag on November 8–17 (0.51) and on December 3–5 (0.50).

Conclusions

- The drag of the ISS at 5 time intervals was considered.
- The increase in ISS's drag and space weather conditions at selected time intervals were considered.
- The periods of enhanced drag of the ISS, at the decay phase of the 23rd solar cycle (28.03.2005–11.05.2005), were caused by: the joint influence of geoeffective fluxes from coronal holes and CIR (April 4–8, April 11–15), wave ionizing radiation from flare activity (April 29 – May 3). The change of the solar sector on April 11–15 resulted in the planet falling into a high-speed flow from the coronal hole.
- Periods of enhanced drag were caused by high-speed flows from the coronal holes and associated with them changes in the interplanetary magnetic field (January 20–21; January 26–29; February 13–18) at the minimum of solar activity (16.01.2009–17.03.2009). The periods February 21 – March 3 and March 5–7 could not be accurately associated with specific manifestations of solar and geomagnetic activity. Perhaps the period of March 5–7 was the result of the weak geomagnetic storm on March 3, which was the reaction to the change in the state of the interplanetary environment as a result of being in high-speed flow from a coronal hole.
- The main parameter influencing the change in the motion of the ISS in the Earth's atmosphere were high-speed streams from coronal holes, which caused changes in the parameters of the solar wind at the minimum of solar activity (31.03.2009–28.06.2009). These changes led to the increase in geomagnetic activity (April 7–10, April 16–22, May 13–18). In the period from April 16 to April 22, the disturbances caused by the flow of the coronal hole subsided by April 18–19, but the drag of the ISS continued to intensify until April 22. It was not possible to ascertain the reason for this effect (perhaps it was a late response of the atmosphere to disturbing events of solar and geomagnetic activity that had occurred earlier). The period of May 28–31 can be associated with an increase in the parameters of the solar wind, which led to the arrival of a shock

wave in the near-Earth space. The periods of drag after May 31 could not be associated with the phenomena of solar and geomagnetic activity.

- The period of enhanced drag (September 19–26) at the phase of the first maximum of the 24 solar activity cycle (15.09.2012–04.10.2012) was caused by the combined effect of the coronal mass ejection (CIR) that reached the Earth and the high-speed flow from the coronal hole, which became geoeffective after the planet crosses the solar sector. The ISS did not react to the arrival of CME and two shock waves from it on September 30. This may be due to the undocking of the planned mission on September 28 and subsequent maneuvers of the station.
- The main events of enhanced drag of the ISS (during the period of 03.11.2012–16.12.2012) were caused by the M-class flare activity (November 8–17, November 29 – December 1), associated with them geoeffective CMEs (November 8–17) and crossing the boundaries of the solar sectors on November 6 and 14. The change in solar sectors led to the increase in the parameters of the solar wind (November 6) and the appearance of a high-speed flow from the coronal hole (November 14). The increase in the ISS's drag coefficient on December 3–5 was caused by the high-speed flow of the coronal hole.
- The main influencing phenomena of solar activity on the change in the drag coefficient during the decay of the 23-rd solar activity cycle and the minimum between the cycles were high-speed streams of coronal holes, which caused changes in the parameters of the solar wind, and recorded (rare) interactions with geoeffective co-rotating interaction regions. At the phase of the first maximum of the 24 solar activity cycle, flare activity and regular geoeffective CMEs are added to the above phenomena.
- For a more correct consideration of the dependence of the ISS drag and space weather, it is planned to build multiple correlation models.

References

1. Shupletsov V. I. 22.06.2014, International Space Station. Orbit tremors [Web resource] // Space Research Laboratory of Ulyanovsk State University. URL: http://www.spacephys.ru/mezhdunarodnaya-kosmicheskaya-stantsiya-drozh-orbity
2. Shupletsov V. I. 24.11.2014, ISS orbit – an indicator of the state of the atmosphere [Web resource] // Space Research Laboratory of Ulyanovsk State University. URL: http://www.spacephys.ru/orbita-mks-indikator-sostoyaniya-atmosfery
3. Mendaza T., Blanco-Avalos J. J., Martin-Torres J. Interplanetary Coronal Mass Ejection effects on thermospheric density as inferred from International Space Station orbital data. Advances in Space Research Volume 60, Issue 10, 15 November 2017, Pages 2233-2251.
4. Beletsky V. V. The movement of an artificial satellite relative to the center of mass. M., 1965, 416 p.
5. Roy A. Orbital movement. M., 1981, 544 p.
6. Kelso T. 1998, Frequently Asked Questions: Two-Line Element Set Format, [Web resource] // CelesTrak. URL: https://celestrak.com/columns/v04n03

7. Felix R. Hoots, Ronald L. Roehrich. Models for Propagation of NORAD Element Sets // Spacetrack Report № 3, December 1988.
8. Vallado, David A.; Paul Crawford; Richard Hujsak; Kelso T. S. "Revisiting Spacetrack Report No 3. // Astrodynamics Specialist Conference. April 29. 2017.
9. J Picone J. M., Emmert J. T. and Lean J. L. Thermospheric densities derived from spacecraft orbits: Accurate processing of two-line element sets // Journal of Geophysical Research, Vol. 110, A03301, 2005.
10. Komendant V. H., Koshkin N. I., Ryabov M. I., Sukharev A. L.Influence effects of space weather on the upper atmosphere according to the drags of artificial earth satellites. Odessa Astronomical Publications, Vol. 27, Issue 1, 2014, p. 89-90.
11. Komendant V. H., Koshkin N. I., Ryabov M. I., Sukharev A. L. Study of quasi-periodic variations in drag of artificial satellite during 23-24 solar cycles. Odessa Astronomical Publications Vol. 28, Issue 2, 2015, p. 277-281.
12. Komendant V. H., Koshkin N. I., Ryabov M. I., Sukharev A. L. Space weather and its influence on the drag dynamics of Earth artificial satellites in 24 solar cycle. Odessa astronomical publications, 2016, Vol. 29, Issue 2, p. 207-210.
13. Komendant V. H. On the character of an artificial satellite drag under various states of solar and geomagnetic activity. Radio Physics and Radio Astronomy. 2020, Vol.25, No 4, p. 308-323.
14. Archive data of artificial satellites TLE elements NORAD. URL: `https://celestrak.com/NORAD/archives/`